HHS Public Access

Author manuscript

Cell Rep. Author manuscript; available in PMC 2017 December 14.

Published in final edited form as:

Cell Rep. 2017 December 05; 21(10): 2737–2747. doi:10.1016/j.celrep.2017.11.048.

Alpha2delta-1 in SF1^{+} Neurons of the Ventromedial Hypothalamus Is an Essential Regulator of Glucose and Lipid Homeostasis

Jennifer A. Felsted[1], **Cheng-Hao Chien**[2], **Dongqing Wang**[3], **Micaella Panessiti**[4], **Dominique Ameroso**[4], **Andrew Greenberg**[1,5], **Guoping Feng**[3], **Dong Kong**[2,4], and **Maribel Rios**[2,4,6,*]

[1]Graduate Program in Biochemical and Molecular Nutrition, Friedman School of Nutrition Science and Policy, Tufts University, Boston, MA 02111, USA

[2]Department of Neuroscience, Tufts University School of Medicine, Boston, MA 02111, USA

[3]McGovern Institute for Brain Research, Department of Brain and Cognitive Sciences, Massachusetts Institute of Technology, Cambridge, MA 02139, USA

[4]Graduate Program in Neuroscience, Sackler School of Graduate Biomedical Sciences, Tufts University School of Medicine, Boston, MA 02111, USA

[5]USDA Human Nutrition Research Center on Aging at Tufts University, Boston, MA 02111, USA

SUMMARY

The central mechanisms controlling glucose and lipid homeostasis are inadequately understood. We show that α2δ-1 is an essential regulator of glucose and lipid balance, acting in steroidogenic factor-1 (SF1) neurons of the ventromedial hypothalamus (VMH). These effects are body weight independent and involve regulation of SF1^{+} neuronal activity and sympathetic output to metabolic tissues. Accordingly, mice with α2δ-1 deletion in SF1 neurons exhibit glucose intolerance, altered lipolysis, and decreased cholesterol content in adipose tissue despite normal energy balance regulation. Profound reductions in the firing rate of SF1 neurons, decreased sympathetic output, and elevated circulating levels of serotonin are associated with these alterations. Normal calcium currents but reduced excitatory postsynaptic currents in mutant SF1 neurons implicate α2δ-1 in the promotion of excitatory synaptogenesis separate from its canonical role as a calcium channel subunit. Collectively, these findings identify an essential mechanism that regulates VMH neuronal activity and glycemic and lipid control and may be a target for tackling metabolic disease.

Graphical abstract

[*]Correspondence: maribel.rios@tufts.edu.
[6]Lead Contact

SUPPLEMENTAL INFORMATION

Supplemental Information includes Supplemental Experimental Procedures and six figures and can be found with this article online at https://doi.org/10.1016/j.celrep.2017.11.048.

AUTHOR CONTRIBUTIONS

J.A.F. performed most of the experiments and data analyses. C.-H.C. and D.K. performed electrophysiological studies. D.W. and G.F. generated the floxed α2δ-1 mice. M.P. performed protein measurements and insulin ELISA. D.A. performed the SF1/α2δ-1 co-localization analysis in VMH. A.G. contributed critical discussion of the data. M.R. designed the study and wrote the manuscript in collaboration with J.A.F. and performed protein measurements.

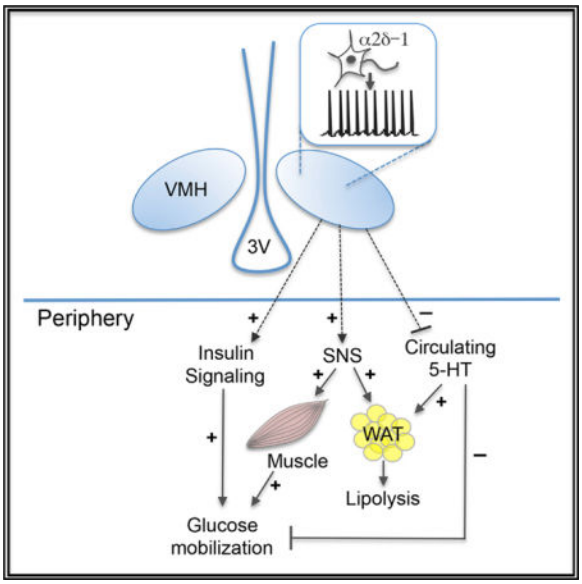

INTRODUCTION

Disorders of energy and glucose balance control have a staggeringly high prevalence worldwide and are associated with a myriad of negative health consequences, including diabetes and cardiovascular disease. Insight into how the brain regulates these physiological processes in coordination with peripheral tissues is paramount in developing effective treatments for these afflictions. Previous investigations implicate the ventromedial hypothalamus (VMH) in the regulation of energy, glucose, and lipid balance (King, 2006; Sudo et al., 1991; Takahashi and Shimazu, 1982) and suggest that these effects are mediated in part by controlling sympathetic output in the periphery (Saito et al., 1989; Takahashi et al., 1994). However, the underlying mechanisms remain largely undefined because this region has been under-studied relative to other hypothalamic nuclei.

Our previous investigations suggested a role of alpha2delta-1 (α2δ-1) in energy and glucose balance control acting downstream of brain-derived neurotrophic factor (BDNF) in the VMH (Cordeira et al., 2014). BDNF signals through the tyrosine kinase B (TrkB) receptor to support neuronal survival, differentiation, and synaptic plasticity (Reichardt, 2006). Notably, BDNF is a key central regulator of energy and glucose homeostasis, and the VMH is a critical target for these actions. Accordingly, diminished BDNF signaling in humans and rodents has been associated with overeating, severe obesity, hyperglycemia, hyperinsulinemia, and hyperlipidemia (Gray et al., 2006, 2007; Han et al., 2008; Liao et al., 2012; Lyons et al., 1999; Rios et al., 2001; Unger et al., 2007; Wang et al., 2007; Xu et al., 2003) α2δ-1, for its part, facilitates cell surface trafficking of calcium channels, mediating calcium currents and neurotransmitter release (Davies et al., 2007). Additionally, α2δ-1 was identified as a receptor for thrombospondins, promoting excitatory synapse assembly via calcium channel-independent mechanisms (Eroglu et al., 2009). However, little is known regarding the relevance of this non-canonical role of α2δ-1, influencing whole-animal physiology.

Here we examined whether α2δ-1 is a requisite factor in the VMH for energy and glucose balance control and whether steroidogenic factor-1 (SF1)-containing neurons are a critical cellular substrate for these actions. SF1 neurons, which are exclusive to this hypothalamic region, are primarily glutamatergic and have established roles in energy and glucose homeostasis regulation (Dhillon et al., 2006; Kim et al., 2012; Klöckener et al., 2011; Tran et al., 2003; Zhang et al., 2008). Despite evidence of these important roles, the mechanisms controlling the activity of these cells are largely unknown. We show that α2δ-1 plays an essential role in regulating the excitability and firing activity of SF1 neurons. Accordingly, its deletion in this cell population leads to neuronal hypoactivity, reduced sympathetic tone to white adipose tissue (WAT) and skeletal muscle, and deficits in glycemic and lipid control. These findings help explain previous reports of metabolic disorders in humans prescribed gabapentinoid drugs that inhibit α2δ-1 function (Gee et al., 1996) to combat neuropathic pain and seizure disorders (DeToledo et al., 1997; Hoppe et al., 2008). Importantly, these results inform a central mechanism controlling glucose and lipid homeostasis.

RESULTS

α2δ-1 in SF1 Neurons Is Not Required for the Regulation of Energy Balance

α2δ-1 is highly expressed in the VMH, particularly in the dorsomedial region, which contains a high density of $SF1^+$ neurons, a cell population that, in the brain, is exclusive to the VMH (Kurrasch et al., 2007; Taylor and Garrido, 2008). Prior reports showed that α2δ-1 promotes excitatory synapse assembly in a calcium-independent manner in other brain regions (Eroglu et al., 2009). Therefore, we hypothesized that α2δ-1 facilitates energy and glucose balance control by increasing the excitatory drive of SF1 neurons. Immunolabeling studies in reporter mice with SF1-cre-dependent expression of GFP revealed extensive co-localization of α2δ-1 and GFP in the VMH, confirming that α2δ-1 is expressed in SF1 neurons (Figure 1A). SF1 neurons lacking α2δ-1 and cells expressing α2δ-1 but not SF1 were also observed in the VMH (Figure 1A; Figure S1). Accordingly, confocal image analysis revealed that, although 67.8% ± 13.6% of SF1 neurons contain α2δ-1, 77.3% ± 3.0% of $\alpha2\delta\text{-}1^+$ cells in the VMH express SF1.

To directly test the role of α2δ-1 in SF1 neurons, we examined the effect of selectively deleting it in this cell population. Toward this aim, we crossed mice containing loxP sites flanking exon 6 of the α2δ-1 gene with mice expressing cre recombinase under the direction of the SF1 promoter (SF1-Cre mice) (Dhillon et al., 2006) to generate mutants ($\alpha2\delta\text{-}1^{2L/2L:SF1\text{-}Cre}$) and controls ($\alpha2\delta\text{-}1^{2L/2L}$) (Figure 1B). Figure 1C shows that the α2δ-1 protein content in the mutant VMH was significantly decreased and only 53% that of controls. Immunolabeling studies revealed significant α2δ-1 depletion primarily in the dorsomedial VMH, which contains a high density of SF1 neurons (Figure 1D). Co-immunolabeling with anti-α2δ-1 and anti-SF1 showed that cytoplasmic expression of α2δ-1 exhibited by control SF1 neurons was reduced in $\alpha2\delta\text{-}1^{2L/2L:SF1\text{-}Cre}$ mutants (Figure S2). Moreover, α2δ-1 expression was observed in processes in close proximity to SF1 neurons in mutant VMH. Finally, measurements of the VMH area and the density of SF1 neurons in

VMH sections stained with DAPI or immunolabeled with anti-SF1 showed no significant differences in α2δ-1$^{2L/2L:SF1-Cre}$ mice compared with controls (Figures S3A and S3B).

Because SF1 is also expressed in the adrenal glands (Luo et al., 1995a, 1995b), cre-mediated recombination and deletion of α2δ-1 is expected in this tissue in α2δ-1$^{2L/2L:SF1-Cre}$ mice. However, we found that α2δ-1 is not expressed in wild-type adrenal glands, and, thus, its depletion in this region is not a confounding factor (Figure S4A). Accordingly, the serum levels of the adrenal hormone epinephrine were normal in α2δ-1$^{2L/2L:SF1-Cre}$ mice compared with controls, further attesting to normal adrenal function (Figure S4B).

Next we examined the effect of α2δ-1 depletion on energy balance regulation. α2δ-1$^{2L/2L:SF1-Cre}$ mutant mice exhibited normal food intake compared with α2δ-1$^{2L/2L}$ mice (Figure 2A). Additionally, no significant differences in consumption of chow diet (CD) during re-feeding following a prolonged fast were observed between mutants and controls (Figure S5). Consistent with the observed normal feeding behavior, the body weights of α2δ-1$^{2L/2L:SF1-Cre}$ mutant mice were similar to those of controls (Figure 2B). Furthermore, when challenged with a high-fat diet (HFD, 5.56 kcal/g) beginning at 8 weeks of age, mutant mice exhibited similar levels of food intake and body weight as control mice (Figures 2A and 2B).

Body composition measurements in mice fed a CD showed a similar content of lean and fat mass in mutants compared with controls (Figure 2C). Similarly, energy expenditure and locomotor activity were not affected in α2δ-1$^{2L/2L:SF1-Cre}$ mutants (Figure 2D and E). In aggregate, the findings indicate that α2δ-1 expression in SF1 neurons is not required for energy balance regulation.

α2δ-1 Deletion in SF1 Neurons Elicits Deficits in Glucose Homeostasis

The VMH is a key glucose-sensing region of the brain facilitating glycemic control (Kang et al., 2006; Song et al., 2001). Therefore, we investigated whether α2δ-1 depletion in SF1 neurons affected glucose homeostasis. Baseline fasting levels of circulating glucose or insulin were not significantly different between α2δ-1$^{2L/2L:SF1-Cre}$ and α2δ-1$^{2L/2L}$ mice on a CD (Figures 3A and 3B). However, α2δ-1$^{2L/2L:SF1-Cre}$ mutants exhibited significantly impaired responses to a glucose challenge compared with controls (Figure 3C and 3D).

Consistent with the findings in the glucose tolerance test, we found that α2δ-1$^{2L/2L:SF1-Cre}$ mice exhibited insulin resistance, as indicated by a blunted decrease in blood glucose following an insulin challenge relative to α2δ-1$^{2L/2L}$ mice (Figure 3E). Accordingly, there was a significant interaction of time and genotype ($p = 0.003$) and a significant increase in glucose levels in mutants compared with controls 15 min following insulin administration (Figure 3E). However, counterregulatory responses to insulin-induced hypoglycemia appeared to be intact in α2δ-1$^{2L/2L:SF1-Cre}$ mutant mice (Figures 3E and 3F). Our findings indicate an essential role of α2δ-1 in SF1 neurons regulating glucose homeostasis.

α2δ-1$^{2L/2L:SF1-Cre}$ Mutants Exhibit Alterations in Lipid Homeostasis

The VMH is known to influence peripheral lipid metabolism, but the underlying mechanisms are poorly understood (Kumon et al., 1976; Ruffin and Nicolaidis, 1999). We

investigated whether α2δ-1 activity in SF1 neurons might play a part. For this, we measured triacylglycerol (TAG) and total cholesterol content in the liver, WAT, and serum of α2δ-$1^{2L/2L:SF1\text{-}Cre}$ mutants and α2δ-$1^{2L/2L}$ controls fed a CD or following a 24-hr fast. Serum, liver, and WAT levels of TAG were not significantly different between genotypes under fed or fasted conditions (Figures 4A–4C). Serum and liver levels of cholesterol were also normal (Figures 4D and 4F). However, there were significant effects of genotype ($p < 0.0003$) and feeding status ($p < 0.01$) on total cholesterol levels in WAT, with fed and fasted mutants exhibiting significant decreases compared with α2δ-$1^{2L/2L}$ control mice (Figure 4E). Moreover, examination of fatty acid profiles revealed modest but significant alterations in liver but not in WAT tissue in both fed and fasted α2δ-$1^{2L/2L:SF1\text{-}Cre}$ mutant mice, suggesting alterations in hepatic lipid homeostasis (Figures 4G and 4H and data not shown).

We investigated potential alterations in lipolysis within WAT. Lipolysis is normally enhanced during conditions of negative energy balance to hydrolyze triglycerides and elevate free fatty acids and glycerol release from adipose tissue, providing the animal with substrates for oxidative metabolism and ATP production in peripheral tissues. No differences in serum non-esterified free fatty acid (NEFA) concentrations were observed under fed or fasted conditions or in serum glycerol levels under fasted conditions (Figures 5A and 5B). However, there was a significant interaction between feeding status and genotype ($p = 0.02$) and a 315% elevation in circulating levels of glycerol in fed mutant mice compared with fed controls, indicating that lipolysis suppression in the fed state was impaired in mutants (Figure 5B). Consistent with increased levels of lipolysis, α2δ-$1^{2L/2L:SF1\text{-}Cre}$ mutants exhibited a modest but significant reduction in adipocyte size (Figures 5C and 5D). To ascertain mechanisms underlying increased lipolysis in fed α2δ-$1^{2L/2L:SF1\text{-}Cre}$ mutants, we measured levels of total, activated ($pHSL_{S660}$), and inhibited ($pHSL_{S565}$) levels of the lipolytic enzyme hormone sensitive lipase (HSL) (Haemmerle et al., 2002) in control and mutant WAT under fed and fasted conditions. Consistent with elevated levels of serum glycerol in fed but not in fasted mutants, there was a trend ($p = 0.06$) toward a significant increase in $pHSL_{S660}$ in WAT in the fed state and normal levels in the fasted state in mutants compared with controls (Figures 5E and 5F and data not shown). The levels of HSL and $pHSL_{S565}$ were normal in both sets of mutants.

To examine potential alterations in adipokine secretion, serum concentrations of leptin and adiponectin were measured. No significant differences were observed between α2δ-$1^{2L/2L:SF1\text{-}Cre}$ and α2δ-$1^{2L/2L}$ mice (Figure S6). In summary, the data indicate that α2δ-1 in SF1 neurons is a critical player in the regulation of lipid balance, influencing activity of lipolytic enzymes in WAT.

α2δ-1 Is a Critical Regulator of SF1 Neuronal Activity

We measured the effect of depleting α2δ-1 on the activity of SF1 neurons using whole-cell recordings to inform central mechanisms leading to dysregulated glucose and lipid balance in α2δ-$1^{2L/2L:SF1\text{-}Cre}$ mice. Control and mutant mice were generated with selective, cre-dependent expression of red fluorescent tdTomato in SF1 neurons to facilitate the identification of these cells in the VMH. We observed a significant 81% reduction in the firing rate of mutant SF1 neurons compared with controls (Figures 6A and 6B). Moreover,

mutants had a significantly hyperpolarized membrane potential compared with control mice (Figure 6B).

We asked whether alterations in calcium currents might be responsible for the diminished firing rate of SF1 neurons in α2δ-1$^{2L/2L:SF1\text{-}Cre}$ mice, considering that the canonical role of α2δ-1 is to serve as an auxiliary high-voltage calcium channel subunit (Davies et al., 2007). We found that calcium currents in mutant SF1 neurons were normal (Figure 6C). Average peak amplitude, voltage dependence, and current kinetics were similar in both groups of animals. Another role of α2δ-1 is to mediate excitatory synaptogenesis in a calcium channel-independent manner through interactions with thrombospondins (Eroglu et al., 2009). Thus, we examined whether mutant SF1 neurons might have alterations in their excitatory drive. A significant decrease in frequency but not amplitude of spontaneous excitatory postsynaptic currents (sEPSCs) was observed in mutant cells ($p = 0.03$) (Figures 6D and 6E). Measurements performed in the presence of tetrodotoxin (TTX) to evaluate action potential-independent excitatory events revealed a significant decrease in frequency and normal amplitude of miniature excitatory post synaptic currents (mEPSCs) in SF1 neurons in α2δ-1$^{2L/2L:SF1\text{-}Cre}$ mice (Figure 6F). Interestingly, the frequency data for sEPSCs and mEPSCs suggest that subpopulations of mutant SF1 neurons might be differentially affected. Accordingly, the VMH of α2δ-1$^{2L/2L:SF1\text{-}Cre}$ mutants contained a subgroup of SF1 neurons exhibiting a frequency of sEPSCs and mEPSCs below 2 Hz that was absent in control VMH (Figures 6G and 6H). Notably, this putative mutant subpopulation was significantly different from another subgroup of mutant cells with a frequency of sEPSCs and mEPSCs above 2 Hz (Figures 6G and 6H) that exhibited levels of activity similar to those of wild-type cells. Finally, we found that the frequency and amplitude of spontaneous inhibitory post synaptic currents (sIPSCs) and miniature inhibitory post synaptic currents (mIPSCs) in SF1 neurons were similar in control and mutant mice (Figures 6I and 6J), indicating that α2δ-1 is not required for the regulation of inhibitory transmission in SF1 neurons.

In aggregate, these data indicate that α2δ-1 plays a critical role in regulating the activity of SF1 neurons through calcium channel-independent mechanisms that increase the excitatory drive onto these cells.

α2δ-1 Depletion in SF1 Neurons Reduces the Sympathetic Tone and Increases Circulating Levels of Serotonin

The VMH can affect peripheral glucose and lipid metabolism through the regulation of sympathetic output to metabolic organs (Saito et al., 1989; Satoh et al., 1999; Shimazu et al., 1991). Thus, we hypothesized that hypoactivity of SF1 neurons in α2δ-1$^{2L/2L:SF1\text{-}Cre}$ mutants might result in decreased sympathetic output, triggering glucose intolerance and disrupted lipid homeostasis. To test this, we measured norepinephrine (NE) concentrations in the liver, WAT, brown adipose tissue (BAT), skeletal muscle, and serum of α2δ-1$^{2L/2L:SF1\text{-}Cre}$ mutant and α2δ-1$^{2L/2L}$ control mice. Whereas NE levels in WAT were depleted by 45% in mutants compared with controls, serum levels were only 27% of those in controls (Figure 7A). No differences in NE content were observed in the liver, BAT, or skeletal muscle. Additionally, levels of the NE metabolite dihydroxylphenylglycol (DHPG),

which is produced following neuronal reuptake of released NE and closely reflects sympathetic activity (Izzo et al., 1985), was significantly decreased in skeletal muscle of α2δ-1$^{2L/2L:SF1-Cre}$ mutant mice relative to controls (Figure 7B).

The elevated levels of lipolysis observed in α2δ-1$^{2L/2L:SF1-Cre}$ mutants (Figures 5B, 5E, and 5F) were counterintuitive considering the significant reduction in sympathetic tone to WAT they exhibit and that NE promotes this process. Previous investigations demonstrated that serotonin (5-HT), another monoamine produced in the periphery by enterochromaffin cells, robustly induces lipolysis via activation of 5-HT$_{2B}$ receptors in WAT (Sumara et al., 2012). Thus, we asked whether alterations in peripheral 5-HT might contribute to abnormal lipid metabolism and glycemic control in the mutants. Measurements showed a significant 2.3-fold elevation in serum 5-HT and normal levels of the metabolite 5-hydroxyindoleacetic acid (5-HIAA) in α2δ-1$^{2L/2L:SF1-Cre}$ mutants compared with α2δ-1$^{2L/2L}$ controls (Figure 7C). These results indicate that α2δ-1 depletion in SF1 neurons leads to blunted sympathetic output and severely increased levels of 5-HT in the periphery, suggesting pathological mechanisms leading to observed alterations in glucose homeostasis and lipid metabolism.

DISCUSSION

Here we demonstrate an essential role of α2δ-1 in regulating the activity of SF1 neurons in the VMH and sympathetic output to metabolic tissues. These studies illustrate a weight-independent mechanism acting in the brain to regulate glycemic control and lipid metabolism. Notably, these actions of α2δ-1 involve effects on the excitatory drive of SF1 neurons and not its canonical calcium channel function. Furthermore, these data reveal a candidate pathological mechanism leading to alterations in glycemic control in lean individuals and patients treated with gabapentinoid drugs, which inhibit α2δ-1 (DeToledo et al., 1997; Gee et al., 1996; Hoppe et al., 2008).

A comprehensive analysis of α2δ-1$^{2L/2L:SF1-Cre}$ mutant mice indicated that α2δ-1 is not required for the regulation of energy balance. This observation was surprising considering our previous finding that rescuing an α2δ-1 deficit broadly in the VMH of adult mice with central BDNF depletion mitigated their hyperphagic behavior and obesity (Cordeira et al., 2014). There are several potential explanations for this discrepancy. Notably, the VMH is comprised of a heterogeneous population of neurons (McClellan et al., 2006), and our immunolabeling studies indicate that α2δ-1 is not exclusively localized to SF1 neurons in this region. Therefore, it is possible that cells in the VMH lacking SF1 are targets of metabolic actions of α2δ-1 influencing energy balance control. It is also possible that deleting α2δ-1 in SF1 neurons during early development triggers compensatory mechanisms that are absent in the mature brain and that partially mitigate the ensuing deleterious effects. Alternatively, the prior observed effects of α2δ-1 gene delivery to the VMH of adult BDNF mutants on energy balance may represent a gain of function.

Despite exhibiting normal energy balance regulation, α2δ-1$^{2L/2L:SF1-Cre}$ mutants are glucose-intolerant, indicating an essential and body weight-independent role of α2δ-1 facilitating glycemic control. Reduced peripheral levels of NE and altered responses during the insulin tolerance test suggest that reduced sympathetic tone and sensitivity to insulin in

metabolic organs contribute to this deficit. Notably, reduced SF1 neuronal activity in mutant mice is a plausible central mechanism driving these pathologies. In support, activating SF1 neurons in mice via designer receptors exclusively activated by designer drugs (DREADD) technology elevated insulin sensitivity and glucose uptake in the periphery (Coutinho et al., 2017). Furthermore, the VMH regulates sympathetic outflow, which, for its part, facilitates glucose uptake by skeletal muscle, WAT, and BAT, and some of these effects are insulin-independent (Kang et al., 2004; Song et al., 2001; Minokoshi et al., 1999; Shiuchi et al., 2009; Tiniakos et al., 1996; Carreño and Seelaender, 2004; Bruinstroop et al., 2012; Abe et al., 1993; Liu et al., 1996). Importantly, electrical stimulation of the VMH increased glucose uptake in skeletal muscle and brown adipose tissue in rats, and this effect was abolished by sympathetic denervation, implicating changes in sympathetic tone (Shimazu et al., 1991; Sudo et al., 1991). Considering these findings, SF1 neuronal hypoactivity and concomitant decreases in sympathetic tone in $\alpha 2\delta\text{-}1^{2L/2L:SF1\text{-}Cre}$ mutants are expected to contribute to abnormal glycemic control.

Reduced SF1 neuronal activity in $\alpha 2\delta\text{-}1^{2L/2L:SF1\text{-}Cre}$ mutants did not appear to compromise counterregulatory responses to hypoglycemia. In contrast, a previous study indicated that chemogenic silencing of SF1 neurons impaired restorative responses to glucoprivation mediated by activation of cholecystokinin $(CCK)^{+}$ cells in the parabrachial nucleus (Garfield et al., 2014). These findings suggest functional diversity in SF1 neurons and that $\alpha 2\delta\text{-}1^{+}$ and CCK-responsive $SF1^{+}$ cells in the VMH might represent distinct subpopulations. Further evidence of heterogeneity in $SF1^{+}$ neurons comes from a recent report indicating that the VMH contains both leptin-activated and leptin-inhibited SF1 neurons (Sohn et al., 2016). These findings are reminiscent of the functional diversity reported in proopiomelanocortin (POMC) neurons of the arcuate nucleus (Sohn et al., 2011; Williams et al., 2010) and illustrate the complexity of neural circuits influencing metabolic function. In support of this idea, our electrophysiology data suggest that the VMH of in $\alpha 2\delta\text{-}1^{2L/2L:SF1\text{-}Cre}$ mutants contains two putative subpopulations of SF1 neurons with reduced or similar levels of activity compared with control cells.

Dysregulated glycemic control in $\alpha 2\delta\text{-}1^{2L/2L:SF1\text{-}Cre}$ mutants was accompanied by decreased cholesterol content in WAT and increased lipolysis in the fed state, indicative of aberrant lipid homeostasis. Previous investigations indicate that alterations in cholesterol levels greatly affect adipocyte metabolic activity, which can ultimately have deleterious effects on insulin sensitivity (Le Lay et al., 2001). The failure of mutants to suppress lipolysis in the fed state was surprising because NE is known to stimulate this process, and mutants exhibited decreased sympathetic tone in WAT. However, these seemly discrepant findings could be explained by the 2.3-fold elevation in circulating 5-HT observed in mutants. In support, mice with selective gut deletion of tryptophan hydroxylase, the rate-limiting enzyme for 5-HT synthesis, exhibited both reduced peripheral 5-HT and impaired lipolysis while having normal body weights, food intake, and circulating triglyceride levels (Sumara et al., 2012). Notably, wild-type mice implanted with 5-HT-releasing pellets to increase the levels of peripheral 5-HT by 2.5-fold exhibited elevated levels of serum glycerol in the fed state and of the lipolytic enzyme $pHSL_{S660}$ in WAT, reminiscent of $\alpha 2\delta\text{-}1^{2L/2L:SF1\text{-}Cre}$ mutants. These effects of 5-HT are mediated by direct action on $5\text{-}HT_{2B}$ receptors on adipocytes. Sumara et al. (2012) also found that peripheral serotonin promotes

hepatic gluconeogenesis and prevents glucose uptake by hepatocytes. Therefore, elevated circulating levels of serotonin evident in α2δ-1$^{2L/2L:SF1\text{-}Cre}$ mutants are expected to also contribute to alterations in glycemic control. It remains unclear whether elevated serum 5-HT in mutants is a primary effect of deleting α2δ-1 in the VMH or a secondary consequence.

The collective data indicate that α2δ-1 is a critical regulator of SF1 neuronal activity. α2δ-1 serves dual roles as a voltage-gated calcium channel subunit and as a receptor for thrombospondins (TSPs), facilitating excitatory synapse assembly (Davies et al., 2007; Eroglu et al., 2009). The calcium currents of SF1^{+} neurons in α2δ-1$^{2L/2L:SF1\text{-}Cre}$ mice were indistinguishable from those of controls. In contrast, the frequency of sEPSCs and mEPSCs was significantly reduced in mutant SF1^{+} neurons, indicating that the latter is the mechanism at play. In agreement, cortical neurons in transgenic mice overexpressing $\alpha_2\delta$-1 exhibited increased density of excitatory synapses and elevated frequency of miniature EPSCs compared with wild-type mice (Eroglu et al., 2009). Conversely, the $\alpha_2\delta$-1 inhibitor gabapentin blocked the positive effects of TSP/$\alpha_2\delta$-1 on excitatory synaptogenesis, whereas calcium channel blockers had no effect, further attesting to the calcium-independent actions of $\alpha_2\delta$-1. Finally, Eroglu et al. (2009) showed that α2δ-1 does not influence inhibitory neurotransmission, consistent with our observation that sIPSCs and mIPSCs were normal in α2δ-1$^{2L/2L:SF1\text{-}Cre}$ mutants. Considering the collective data, it is possible that α2δ-1 mediates contact of excitatory presynaptic terminals originating within or outside the VMH onto SF1 neurons to increase their activity.

In summary, we demonstrate a requisite role of α2δ-1 regulating SF1 neuronal activity and metabolic function. We propose that α2δ-1 action through non-canonical mechanisms increases the excitatory drive and activity of SF1 neurons, mediating increased sympathetic output to metabolic organs to achieve glucose homeostasis. Additionally, α2δ-1 might act on SF1 neurons to negatively regulate serotonin production in the periphery, ultimately affecting lipid metabolism in WAT. The collective findings inform pathological mechanisms underlying metabolic disturbances in individuals administered the anti-epileptic and anti-nociceptive drugs gabapentin and pregabalin, which bind and inhibit $\alpha_2\delta$-1 (DeToledo et al., 1997; Hoppe et al., 2008). They are interesting, considering a recent human study showing that an individual with a *de novo* chromosomal truncation encompassing *CACNA2D1*, the gene encoding $\alpha_2\delta$-1, exhibited metabolic alterations, including hyperinsulism (Vergult et al., 2014). Because this truncation also involved deletion of the metabolic gene *CD36*, the authors speculated that metabolic alterations were elicited by that deficit. However, the possibility of $\alpha_2\delta$-1 involvement cannot be ruled out. Therefore, further defining the mechanistic consequences of central α2δ-1 action is an essential step in creating avenues to tackle metabolic disorders, including diabetes.

EXPERIMENTAL PROCEDURES

Animals

All procedures were approved by the Institutional Animal Care and Use Committee at Tufts University and conducted in accordance with NIH Guide for Care and Use of Laboratory Animals guidelines. Mice with specific α2δ-1 depletion in SF1-positive neurons of the

VMH were generated by crossing floxed α2δ-1 mice with SF1-Cre transgenic mice obtained from The Jackson Laboratory (stock no. 012462, Tg(Nr5a1-cre)7Lowl/J), and they were in a C57BL/6J-129 hybrid background (Dhillon et al., 2006). Unless otherwise indicated, male α2δ-$1^{2L/2L}$ (control) and α2δ-$1^{2L/2L:SF1\text{-}Cre}$ (mutant) mice, 18–20 weeks of age and fed a chow diet, were used for the studies described throughout the manuscript. For the electrophysiology experiments, mice containing the floxed α2δ-1 and SF1-cre alleles were crossed to mice with mice with cre-dependent expression of tdTomato (stock no. 007914, B6.Cg-Gt(ROSA)26$Sor^{tm14(CAG\text{-}tdTomato)Hze}$/J), obtained from The Jackson Laboratory.

Immunofluorescence

Thirty-micron-thick free-floating coronal sections were immunolabeled with mouse anti-α2δ-1 (1:100, Sigma, St. Louis, MO) and/or anti-SF1 (1:200, TransGenic, Tokyo, Japan) diluted in blocking solution. A Nikon A1R microscope configured for confocal microscopy was used to capture images of labeled brain sections. Co-localization of SF1 and α2δ-1, measurements of VMH area, and SF1 cell density were quantified using NIH ImageJ.

Western Blot Analysis

Western blot analysis of samples was conducted using standard methods. Blot images were acquired usinga Fujifilm LAS-4000image reader, and densitometry was performed using Quantity One analysis software (Bio-Rad, Hercules, CA). The following primary antibodies were used: mouse anti-α2δ-1 (1:750, Sigma, St. Louis, MO), mouse anti-b-tubulin (1:10,000, Sigma, St. Louis, MO), rabbit anti-HSL, anti-$pHSL_{S660}$, or anti-$pHSL_{S565}$ (1:1,000, Cell Signaling Technology, Danvers, MA), and mouse anti-actin (1:10,000; Thermo Fisher Scientific).

Electrophysiology

Electrophysiology was performed as described previously (Kong et al., 2012). Briefly, 300-μm-thick coronal sections were cut with a Leica VT1000S vibratome and then incubated in carbogen-saturated (95% O_2/5% CO_2) artificial cerebrospinal fluid (ACSF) (125 mM NaCl, 2.5 mM KCl, 1 mM $MgCl_2$, 2 mM $CaCl_2$, 1.25 mM NaH_2PO_4, 25 mM $NaHCO_3$, and 10 mM glucose) at 34°C for 30–45 min before recording. All recordings were obtained within 4 hr of slicing at room temperature. Whole-cell recordings were made on identified neurons under infrared-differential interference contrast (IR-DIC) optics using a MultiClamp 700B amplifier (Axon Instruments) with home-programmed software based on MATLAB. Recording electrodes had resistances of 3–5 mega-ohm (MU). For current clamp recordings, K^+ internal solution was used, which contained 135 mM $KMeSO_3$, 3 mM KCl, 10 mM 4-(2-hydroxyethyl)-1-piperazineethanesulfonic acid (HEPES), 1 mM EGTA, 0.1 mM $CaCl_2$, 4 mM Mg-ATP, 0.3 mM Na-guanosine triphosphate (GTP), and 8 mM Na_2-phosphocreatine (pH 7.3 adjusted with KOH, 295 mOsm·kg^{-1}). Membrane potential and action potential firing were recorded for ~3 min and averaged ~3 minutes after successfully patching onto the neurons. Membrane potentials were corrected offline for an ~8-mV liquid junction potential. For voltage-clamp recordings, Cs^+ internal solution containing 135 mM $CsMeSO_3$, 10 mM HEPES, 1 mM EGTA, 3.3 mM QX-314 (Cl^- salt), 4 mM Mg-ATP, 0.3 mM Na-GTP, and 8 mM Na_2-phosphocreatine (pH 7.3 adjusted with CsOH, 295 mOsm·kg^{-1}) was used. Data were filtered at 3 kHz and sampled at 10 kHz. Series resistance,

measured with a 5-mV hyperpolarizing pulse in voltage clamp, was on average under 20 MU and less than 25 MU, uncompensated. For current-clamp recordings, membrane potentials were corrected for an ~8-mV liquid junction potential. For sEPSC recording, neurons were held at 60 mV, and regular ACSF was added with bicuculline (10 μM) to block ionotropic GABAergic currents.

For the voltage-clamp recording of Ca^{2+} currents, recording electrodes had resistances of 3–5 MU and were filled with the Cs^{+} internal solution described above. Regular ACSF was added, containing the following: 5 mM 4-aminopyridine (4-AP), 5 mM CsCl, 10 mM tetraethylammonium chloride (TEA-Cl), and 0.0005 TTX. Bicuculline (10 μM), 2-amino-5-phosphonovaleric acid (APV) (50 μM), and 2,3-dihydroxy-6-nitro-7-sulfamoyl-benzo(F) quinoxaline (NBQX) (10 μM) were also included in the bath solution to block ionotropic GABAergic and glutamatergic currents. Neuronal membrane potential was held at 70 mV during voltage-clamp recordings, and calcium currents were elicited by a 250-ms depolarizing test pulse from −70 to +50 mV in 10-mV increments. All currents were corrected for leak and capacitive currents offline by a P/-4 protocol. Current density was calculated by dividing the peak current amplitude by membrane capacitance, Cm (picoamperes/picofarads).

Glucose and Insulin Tolerance Tests

For the glucose tolerance test (GTT), mice were fasted for 16 hr, and blood droplets were collected from a lateral tail nick to measure glucose using the Freestyle blood glucose monitoring system (Abbot Diabetes Care, Alameda, CA) at baseline and following administration of 1.5 g/kg of D-glucose. For the insulin tolerance test (ITT), animals were fasted for 6 hr, followed by blood glucose measurements at baseline and following intraperitoneal administration of 0.75 U/kg insulin (Human-R Insulin (rDNA) U100, Lilly).

Tissue Collection and Measurements

Animals were euthanized, and tissues were dissected and flash-frozen in liquid nitrogen. Serum insulin (insulin ELISA kit, Mercodia), leptin (mouse leptin ELISA kit, Millipore), adiponectin (mouse adiponectin ELISA kit, Millipore), NEFAs (HR Series NEFA-HR(2) kit, Wako Diagnostics), and glycerol (free glycerol reagent, Sigma) were measured using commercially available kits. Triglyceride and total cholesterol concentrations were determined by the Van-derbilt Hormone Assay and Analytical Services Core (Vanderbilt University, Nashville, TN). NE, DHPG, serotonin, and 5-HIAA content were measured using high-performance liquid chromatography (HPLC) methods by the Neurochemistry Core Laboratory at the Vanderbilt Brain Institute.

Statistical Analysis

Analytical software used to perform statistical analyses included GraphPad Prism and SAS (Statistical Analysis Software). Repeated-measures ANOVA, using Tukey’s honest significant difference (HSD) to adjust for multiple comparisons, was performed to analyze weekly food intake and body weight measurements as well as the time course data for the glucose and ITTs. Two-way ANOVAs were used to analyze NEFAs, glycerol, triglyceride, and total cholesterol concentrations in control and mutants under fed and fasted conditions.

Student's unpaired t tests were performed to analyze group comparisons for body composition, locomotor activity, energy expenditure, tissue DHPG and NE, serum leptin, serum adiponectin, adipocyte size, and electrophysiology experiments. Comparisons were determined to be statistically significant when $p < 0.05$. All values are depicted as mean ± SEM.

Supplementary Material

Refer to Web version on PubMed Central for supplementary material.

Acknowledgments

These studies were supported by NIH/NIDDK (DK073311) and American Diabetes Association (1-16-IBS-247) grants to M.R., and NIH/NIDDK (R01 DK108797) and NIH/NINDS (R21 NS097922) grants to D.K. J.A.F. and D.A. were supported by NIH Training Grants T32 DK062032 and T32 NS061764, respectively. C.C. was supported by an AHA postdoctoral fellowship (17POST33661185). We thank the core facilities at Tufts University and the Vanderbilt lipid core facility, which are supported by the Tufts Center for Neuroscience Research (P30 NS047243) and Grant DK59637, respectively, for facilitating these studies. We also thank Jean Rivera and Anna Rock for technical assistance.

References

Abe H, Minokoshi Y, Shimazu T. Effect of a beta 3-adrenergic agonist, BRL35135A, on glucose uptake in rat skeletal muscle in vivo and in vitro. J Endocrinol. 1993; 139:479–486. [PubMed: 7907647]

Bruinstroop E, Pei L, Ackermans MT, Foppen E, Borgers AJ, Kwakkel J, Alkemade A, Fliers E, Kalsbeek A. Hypothalamic neuropeptide Y (NPY) controls hepatic VLDL-triglyceride secretion in rats via the sympathetic nervous system. Diabetes. 2012; 61:1043–1050. [PubMed: 22461566]

Carreño FR, Seelaender MC. Liver denervation affects hepatocyte mitochondrial fatty acid transport capacity. Cell Biochem Funct. 2004; 22:9–17. [PubMed: 14695648]

Cordeira JW, Felsted JA, Teillon S, Daftary S, Panessiti M, Wirth J, Sena-Esteves M, Rios M. Hypothalamic dysfunction of the thrombospondin receptor α2δ-1 underlies the overeating and obesity triggered by brain-derived neurotrophic factor deficiency. J Neurosci. 2014; 34:554–565. [PubMed: 24403154]

Coutinho EA, Okamoto S, Ishikawa AW, Yokota S, Wada N, Hirabayashi T, Saito K, Sato T, Takagi K, Wang CC, et al. Activation of SF1 Neurons in the Ventromedial Hypothalamus by DREADD Technology Increases Insulin Sensitivity in Peripheral Tissues. Diabetes. 2017; 66:2372–2386. [PubMed: 28673934]

Davies A, Hendrich J, Van Minh AT, Wratten J, Douglas L, Dolphin AC. Functional biology of the alpha(2)delta subunits of voltage-gated calcium channels. Trends Pharmacol Sci. 2007; 28:220–228. [PubMed: 17403543]

DeToledo JC, Toledo C, DeCerce J, Ramsay RE. Changes in body weight with chronic, high-dose gabapentin therapy. Ther Drug Monit. 1997; 19:394–396. [PubMed: 9263379]

Dhillon H, Zigman JM, Ye C, Lee CE, McGovern RA, Tang V, Kenny CD, Christiansen LM, White RD, Edelstein EA, et al. Leptin directly activates SF1 neurons in the VMH, and this action by leptin is required for normal body-weight homeostasis. Neuron. 2006; 49:191–203. [PubMed: 16423694]

Eroglu C, Allen NJ, Susman MW, O'Rourke NA, Park CY, Ozkan E, Chakraborty C, Mulinyawe SB, Annis DS, Huberman AD, et al. Gabapentin receptor alpha2delta-1 is a neuronal thrombospondin receptor responsible for excitatory CNS synaptogenesis. Cell. 2009; 139:380–392. [PubMed: 19818485]

Garfield AS, Shah BP, Madara JC, Burke LK, Patterson CM, Flak J, Neve RL, Evans ML, Lowell BB, Myers MG Jr, Heisler LK. A parabrachial-hypothalamic cholecystokinin neurocircuit controls counterregulatory responses to hypoglycemia. Cell Metab. 2014; 20:1030–1037. [PubMed: 25470549]

Gee NS, Brown JP, Dissanayake VU, Offord J, Thurlow R, Woodruff GN. The novel anticonvulsant drug, gabapentin (Neurontin), binds to the alpha2delta subunit of a calcium channel. J Biol Chem. 1996; 271:5768–5776. [PubMed: 8621444]

Gray J, Yeo GS, Cox JJ, Morton J, Adlam AL, Keogh JM, Yanovski JA, El Gharbawy A, Han JC, Tung YC, et al. Hyperphagia, severe obesity, impaired cognitive function, and hyperactivity associated with functional loss of one copy of the brain-derived neurotrophic factor (BDNF) gene. Diabetes. 2006; 55:3366–3371. [PubMed: 17130481]

Gray J, Yeo G, Hung C, Keogh J, Clayton P, Banerjee K, McAulay A, O'Rahilly S, Farooqi IS. Functional characterization of human NTRK2 mutations identified in patients with severe early-onset obesity. Int J Obes. 2007; 31:359–364.

Haemmerle G, Zimmermann R, Hayn M, Theussl C, Waeg G, Wagner E, Sattler W, Magin TM, Wagner EF, Zechner R. Hormone-sensitive lipase deficiency in mice causes diglyceride accumulation in adipose tissue, muscle, and testis. J Biol Chem. 2002; 277:4806–4815. [PubMed: 11717312]

Han JC, Liu QR, Jones M, Levinn RL, Menzie CM, Jefferson-George KS, Adler-Wailes DC, Sanford EL, Lacbawan FL, Uhl GR, et al. Brain-derived neurotrophic factor and obesity in the WAGR syndrome. N Engl J Med. 2008; 359:918–927. [PubMed: 18753648]

Hoppe C, Rademacher M, Hoffmann JM, Schmidt D, Elger CE. Bodyweight gain under pregabalin therapy in epilepsy: mitigation by counseling patients? Seizure. 2008; 17:327–332. [PubMed: 18060813]

Izzo JL Jr, Thompson DA, Horwitz D. Plasma dihydroxyphenylglycol (DHPG) in the in vivo assessment of human neuronal norepinephrine metabolism. Life Sci. 1985; 37:1033–1038. [PubMed: 4033349]

Kang L, Routh VH, Kuzhikandathil EV, Gaspers LD, Levin BE. Physiological and molecular characteristics of rat hypothalamic ventromedial nucleus glucosensing neurons. Diabetes. 2004; 53:549–559. [PubMed: 14988237]

Kang L, Dunn-Meynell AA, Routh VH, Gaspers LD, Nagata Y, Nishimura T, Eiki J, Zhang BB, Levin BE. Glucokinase is a critical regulator of ventromedial hypothalamic neuronal glucosensing. Diabetes. 2006; 55:412–420. [PubMed: 16443775]

Kim KW, Donato J Jr, Berglund ED, Choi YH, Kohno D, Elias CF, Depinho RA, Elmquist JK. FOXO1 in the ventromedial hypothalamus regulates energy balance. J Clin Invest. 2012; 122:2578–2589. [PubMed: 22653058]

King BM. The rise, fall, and resurrection of the ventromedial hypothalamus in the regulation of feeding behavior and body weight. Physiol Behav. 2006; 87:221–244. [PubMed: 16412483]

Klöckener T, Hess S, Belgardt BF, Paeger L, Verhagen LA, Husch A, Sohn JW, Hampel B, Dhillon H, Zigman JM, et al. High-fat feeding promotes obesity via insulin receptor/PI3K-dependent inhibition of SF-1 VMH neurons. Nat Neurosci. 2011; 14:911–918. [PubMed: 21642975]

Kong D, Tong Q, Ye C, Koda S, Fuller PM, Krashes MJ, Vong L, Ray RS, Olson DP, Lowell BB. GABAergic RIP-Cre neurons in the arcuate nucleus selectively regulate energy expenditure. Cell. 2012; 151:645–657. [PubMed: 23101631]

Kumon A, Takahashi A, Hara T, Shimazu T. Mechanism of lipolysis induced by electrical stimulation of the hypothalamus in the rabbit. J Lipid Res. 1976; 17:551–558. [PubMed: 993668]

Kurrasch DM, Cheung CC, Lee FY, Tran PV, Hata K, Ingraham HA. The neonatal ventromedial hypothalamus transcriptome reveals novel markers with spatially distinct patterning. J Neurosci. 2007; 27:13624–13634. [PubMed: 18077674]

Le Lay S, Krief S, Farnier C, Lefrère I, Le Liepvre X, Bazin R, Ferré P, Dugail I. Cholesterol, a cell size-dependent signal that regulates glucose metabolism and gene expression in adipocytes. J Biol Chem. 2001; 276:16904–16910. [PubMed: 11278795]

Liao GY, An JJ, Gharami K, Waterhouse EG, Vanevski F, Jones KR, Xu B. Dendritically targeted Bdnf mRNA is essential for energy balance and response to leptin. Nat Med. 2012; 18:564–571. [PubMed: 22426422]

Liu YL, Cawthorne MA, Stock MJ. Biphasic effects of the beta-adrenoceptor agonist, BRL 37344, on glucose utilization in rat isolated skeletal muscle. Br J Pharmacol. 1996; 117:1355–1361. [PubMed: 8882636]

Luo X, Ikeda Y, Lala DS, Baity LA, Meade JC, Parker KL. A cell-specific nuclear receptor plays essential roles in adrenal and gonadal development. Endocr Res. 1995a; 21:517–524. [PubMed: 7588417]

Luo X, Ikeda Y, Parker KL. The cell-specific nuclear receptor steroidogenic factor 1 plays multiple roles in reproductive function. Philos Trans R Soc Lond B Biol Sci. 1995b; 350:279–283. [PubMed: 8570692]

Lyons WE, Mamounas LA, Ricaurte GA, Coppola V, Reid SW, Bora SH, Wihler C, Koliatsos VE, Tessarollo L. Brain-derived neurotrophic factor-deficient mice develop aggressiveness and hyperphagia in conjunction with brain serotonergic abnormalities. Proc Natl Acad Sci USA. 1999; 96:15239–15244. [PubMed: 10611369]

McClellan KM, Parker KL, Tobet S. Development of the ventromedial nucleus of the hypothalamus. Front Neuroendocrinol. 2006; 27:193–209. [PubMed: 16603233]

Minokoshi Y, Haque MS, Shimazu T. Microinjection of leptin into the ventromedial hypothalamus increases glucose uptake in peripheral tissues in rats. Diabetes. 1999; 48:287–291. [PubMed: 10334303]

Reichardt LF. Neurotrophin-regulated signalling pathways. Philos Trans R Soc Lond B Biol Sci. 2006; 361:1545–1564. [PubMed: 16939974]

Rios M, Fan G, Fekete C, Kelly J, Bates B, Kuehn R, Lechan RM, Jaenisch R. Conditional deletion of brain-derived neurotrophic factor in the postnatal brain leads to obesity and hyperactivity. Mol Endocrinol. 2001; 15:1748–1757. [PubMed: 11579207]

Ruffin M, Nicolaidis S. Electrical stimulation of the ventromedial hypothalamus enhances both fat utilization and metabolic rate that precede and parallel the inhibition of feeding behavior. Brain Res. 1999; 846:23–29. [PubMed: 10536210]

Saito M, Minokoshi Y, Shimazu T. Accelerated norepinephrine turnover in peripheral tissues after ventromedial hypothalamic stimulation in rats. Brain Res. 1989; 481:298–303. [PubMed: 2566357]

Satoh N, Ogawa Y, Katsuura G, Numata Y, Tsuji T, Hayase M, Ebihara K, Masuzaki H, Hosoda K, Yoshimasa Y, Nakao K. Sympathetic activation of leptin via the ventromedial hypothalamus: leptin-induced increase in catecholamine secretion. Diabetes. 1999; 48:1787–1793. [PubMed: 10480609]

Shimazu T, Sudo M, Minokoshi Y, Takahashi A. Role of the hypothalamus in insulin-independent glucose uptake in peripheral tissues. Brain Res Bull. 1991; 27:501–504. [PubMed: 1959052]

Shiuchi T, Haque MS, Okamoto S, Inoue T, Kageyama H, Lee S, Toda C, Suzuki A, Bachman ES, Kim YB, et al. Hypothalamic orexin stimulates feeding-associated glucose utilization in skeletal muscle via sympathetic nervous system. Cell Metab. 2009; 10:466–480. [PubMed: 19945404]

Sohn JW, Xu Y, Jones JE, Wickman K, Williams KW, Elmquist JK. Serotonin 2C receptor activates a distinct population of arcuate pro-opiomelanocortin neurons via TRPC channels. Neuron. 2011; 71:488–497. [PubMed: 21835345]

Sohn JW, Oh Y, Kim KW, Lee S, Williams KW, Elmquist JK. Leptin and insulin engage specific PI3K subunits in hypothalamic SF1 neurons. Mol Metab. 2016; 5:669–679. [PubMed: 27656404]

Song Z, Levin BE, McArdle JJ, Bakhos N, Routh VH. Convergence of pre- and postsynaptic influences on glucosensing neurons in the ventromedial hypothalamic nucleus. Diabetes. 2001; 50:2673–2681. [PubMed: 11723049]

Sudo M, Minokoshi Y, Shimazu T. Ventromedial hypothalamic stimulation enhances peripheral glucose uptake in anesthetized rats. Am J Physiol. 1991; 261:E298–E303. [PubMed: 1887876]

Sumara G, Sumara O, Kim JK, Karsenty G. Gut-derived serotonin is a multifunctional determinant to fasting adaptation. Cell Metab. 2012; 16:588–600. [PubMed: 23085101]

Takahashi A, Shimazu T. Hypothalamic regulation of lipid metabolism in the rat: effect of hypothalamic stimulation on lipogenesis. J Auton Nerv Syst. 1982; 6:225–235. [PubMed: 6757306]

Takahashi A, Ishimaru H, Ikarashi Y, Maruyama Y. Aspects of hypothalamic neuronal systems in VMH lesion-induced obese rats. J Auton Nerv Syst. 1994; 48:213–219. [PubMed: 7963256]

Taylor CP, Garrido R. Immunostaining of rat brain, spinal cord, sensory neurons and skeletal muscle for calcium channel alpha2-delta (alpha2-delta) type 1 protein. Neuroscience. 2008; 155:510–521. [PubMed: 18616987]

Tiniakos DG, Lee JA, Burt AD. Innervation of the liver: morphology and function. Liver. 1996; 16:151–160. [PubMed: 8873001]

Tran PV, Lee MB, Marín O, Xu B, Jones KR, Reichardt LF, Rubenstein JR, Ingraham HA. Requirement of the orphan nuclear receptor SF-1 in terminal differentiation of ventromedial hypothalamic neurons. Mol Cell Neurosci. 2003; 22:441–453. [PubMed: 12727442]

Unger TJ, Calderon GA, Bradley LC, Sena-Esteves M, Rios M. Selective deletion of Bdnf in the ventromedial and dorsomedial hypothalamus of adult mice results in hyperphagic behavior and obesity. J Neurosci. 2007; 27:14265–14274. [PubMed: 18160634]

Vergult S, Dheedene A, Meurs A, Faes F, Isidor B, Janssens S, Gautier A, Le Caignec C, Menten B. Genomic aberrations of the CACNA2D1 gene in three patients with epilepsy and intellectual disability. Eur J Hum Genet. 2014; 23:628–632. [PubMed: 25074461]

Wang C, Bomberg E, Levine A, Billington C, Kotz CM. Brain-derived neurotrophic factor in the ventromedial nucleus of the hypothalamus reduces energy intake. Am J Physiol Regul Integr Comp Physiol. 2007; 293:R1037–R1045. [PubMed: 17553842]

Williams KW, Margatho LO, Lee CE, Choi M, Lee S, Scott MM, Elias CF, Elmquist JK. Segregation of acute leptin and insulin effects in distinct populations of arcuate proopiomelanocortin neurons. J Neurosci. 2010; 30:2472–2479. [PubMed: 20164331]

Xu B, Goulding EH, Zang K, Cepoi D, Cone RD, Jones KR, Tecott LH, Reichardt LF. Brain-derived neurotrophic factor regulates energy balance downstream of melanocortin-4 receptor. Nat Neurosci. 2003; 6:736–742. [PubMed: 12796784]

Zhang R, Dhillon H, Yin H, Yoshimura A, Lowell BB, Maratos-Flier E, Flier JS. Selective inactivation of Socs3 in SF1 neurons improves glucose homeostasis without affecting body weight. Endocrinology. 2008; 149:5654–5661. [PubMed: 18669597]

Highlights

- Glycemic and lipid but not energy balance control requires intact α2δ-1 in VMH
- α2δ-1 elevates SF1 neuronal activity through calcium channel-independent mechanisms
- α2δ-1 in VMH positively regulates sympathetic tone to metabolic tissues
- Elevated circulating levels of serotonin result from α2δ-1 depletion in VMH

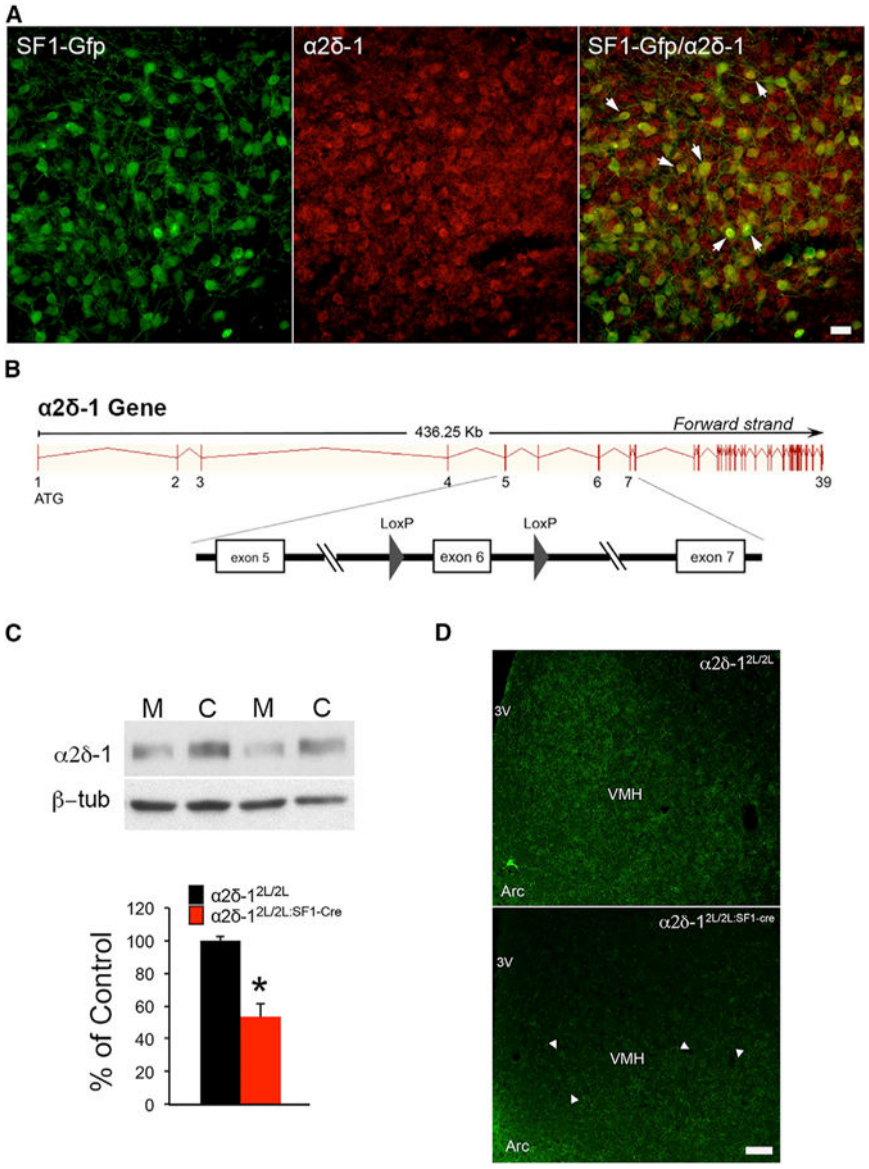

Figure 1. Expression of α2δ-1 in SF1 Neurons of the VMH and Generation of α2δ-1$^{2L/2L:SF1\text{-}Cre}$ Mutant Mice

(A) Immunolabeling of α2δ-1 in GFP-tagged SF1 neurons in the VMH demonstrating co-localization of α2δ-1 and SF1 in the VMH (arrows). Scale bar, 20 μM.

(B) A schematic of the targeting strategy to introduce lox P sites flanking exon 6 of the α2δ-1 gene.

(C) Western blot analysis of α2δ-1 content in the VMH of α2δ-1$^{2L/2L}$ (n = 5) and α2δ-1$^{2L/2L:SF1\text{-}Cre}$ (n = 4) mice. Unpaired, two-tailed t test, *p = 0.001.

(D) α2δ-1 immunolabeling in the hypothalamus of male α2δ-1$^{2L/2L:SF1\text{-}Cre}$ (mutant) and α2δ-1$^{2L/2L}$ (control) mice. Arrowheads denote areas with persistent α2δ-1 expression in the VMH of α2δ-1$^{2L/2L:SF1\text{-}Cre}$ mice. Scale bar, 50 μM.

VMH, ventromedial hypothalamus; Arc, arcuate nucleus; 3V, third ventricle. Data are represented as mean ± SEM. See also Figures S1–S4.

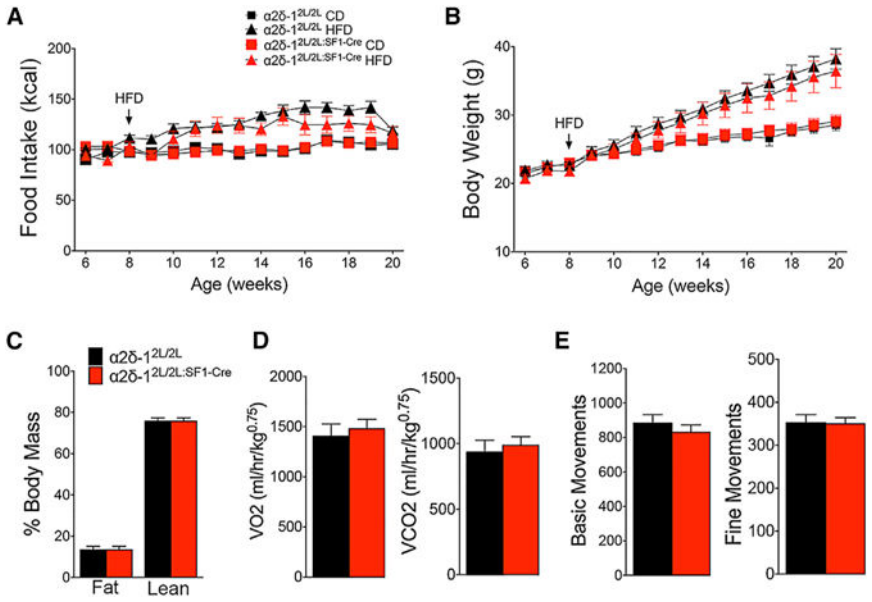

Figure 2. Mice with α2δ-1 Depletion in VMH SF1 Neurons Exhibit Normal Energy Balance Regulation

(A and B) Weekly food consumption (A) and body weight measurements (B) for male α2δ-$1^{2L/2L:SF1\text{-}Cre}$ and α2δ-$1^{2L/2L}$ control mice on a chow diet (CD) or high-fat diet (HFD). Number of animals: α2δ-$1^{2L/2L}$ CD/HFD = 8/11, α2δ-$1^{2L/2L:SF1\text{-}Cre}$ CD/HFD, 9/10.

(C) Body composition measurements in α2δ-$1^{2L/2L:SF1\text{-}Cre}$ and α2δ-$1^{2L/2L}$ mice fed CD at 20 weeks of age (n = 7).

(D) Energy expenditure expressed as average volume of oxygen (VO2; left) and volume of carbon dioxide (VCO2; right) for weight-matched male mice on a chow diet (n = 8).

(E) Home cage locomotor activity expressed as average daily basic (photobeam breaks) and fine movements for α2δ-$1^{2L/2L}$ (n = 13) and α2δ-$1^{2L/2L:SF1\text{-}Cre}$ (n = 18) mice.

Data are represented as mean ± SEM. See also Figure S5.

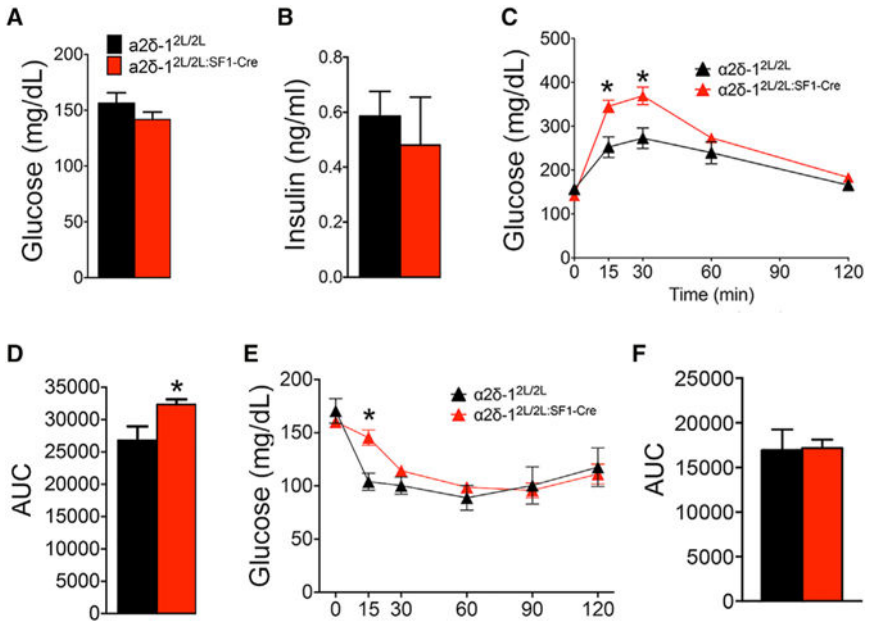

Figure 3. α2δ-1$^{2L/2L:SF1-Cre}$ Mutant Mice Exhibit Deficits in Glucose Homeostasis

(A) Fasting blood glucose levels in α2δ-1$^{2L/2L:SF1-Cre}$ and α2δ-1$^{2L/2L}$ (n = 8) mice on CD.

(B) Fasting serum insulin levels in α2δ-1$^{2L/2L}$ (n = 5) and α2δ-1$^{2L/2L:SF1-Cre}$ (n = 4) mice on CD.

(C) Time course for GTT in α2δ-1$^{2L/2L:SF1-Cre}$ and α2δ-1$^{2L/2L}$ mice on CD (n = 8). Repeated-measures ANOVA, using Tukey's HSD to adjust for multiple comparisons: time, $F(4,70) = 41.7$, $p < 0.0003$; genotype, $F(1,70) = 18.9$, $p < 0.001$; interaction: $F(4, 70) = 4.3$, $p = 0.004$.

(D) Area under the curve (AUC) for GTT. Unpaired, two-tailed t test, *p = 0.03.

(E) Time course for ITT in α2δ-1$^{2L/2L}$ (n = 6) and α2δ-1$^{2L/2L:SF1-Cre}$ (n = 11) mice. Repeated-measures ANOVA, using Tukey's HSD to adjust for multiple comparisons: time, $F(5,75) = 29.7$, $p < 0.0001$; genotype, $F(1,15) = 0.6$, $p < 0.4$; interaction: $F(5, 75) = 4.0$, $p = 0.003$. For the 15 min time point, *p = 0.003.

(F) AUC for ITT. Data are represented as mean ± SEM.

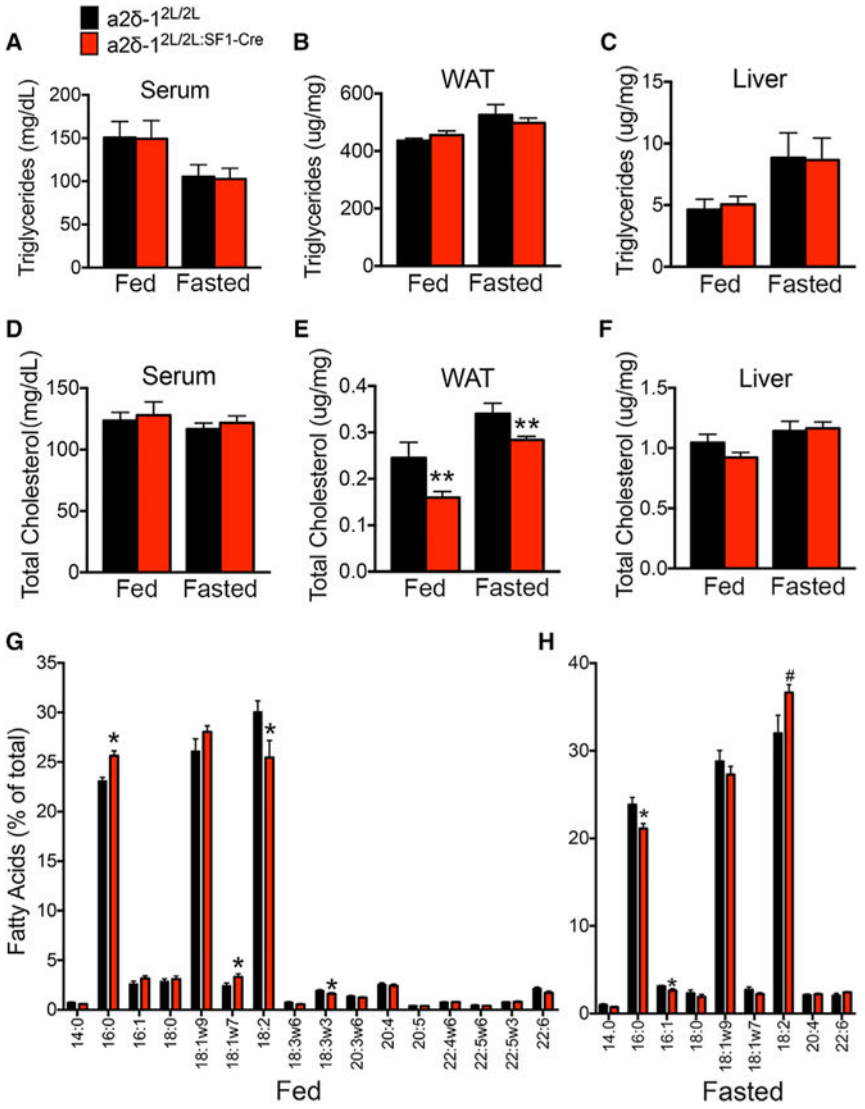

Figure 4. α2δ-1$^{2L/2L:SF1-Cre}$ Mutant Mice Have Alterations in Lipid Balance

(A–C) Levels of triglycerides in serum (A), white adipose tissue (WAT) (B), and liver (C) of α2δ-1$^{2L/2L}$ mice (fed, n = 8; fasted, n = 5) and α2δ-1$^{2L/2L:SF1-Cre}$ (fed, n = 7; fasted, n = 5).

(D–F) Levels of cholesterol in serum (D), WAT (E), and liver (F) of α2δ-1$^{2L/2L}$ mice (fed, n = 8; fasted, n = 5) and α2δ-1$^{2L/2L:SF1-Cre}$ (fed, n = 7; fasted, n = 5). **p = 0.04. Two-way ANOVA: WAT cholesterol: feeding status, F(1,21) = 18.4, p = 0.0003; genotype, F(1,21) = 7.6, p = 0.01; interaction: F(1,21) = 0.32, p = 0.58.

(G and H) Liver fatty acid profiles in fed (G) and fasted (E) α2δ-1$^{2L/2L}$ (fed, n = 8; fasted, n = 5) and α2δ-1$^{2L/2L:SF1-Cre}$ (fed, n = 7; fasted, n = 5) mice.

Two-tailed unpaired t test: *p < 0.05, #p = 0.07.

Data are represented as mean ± SEM.

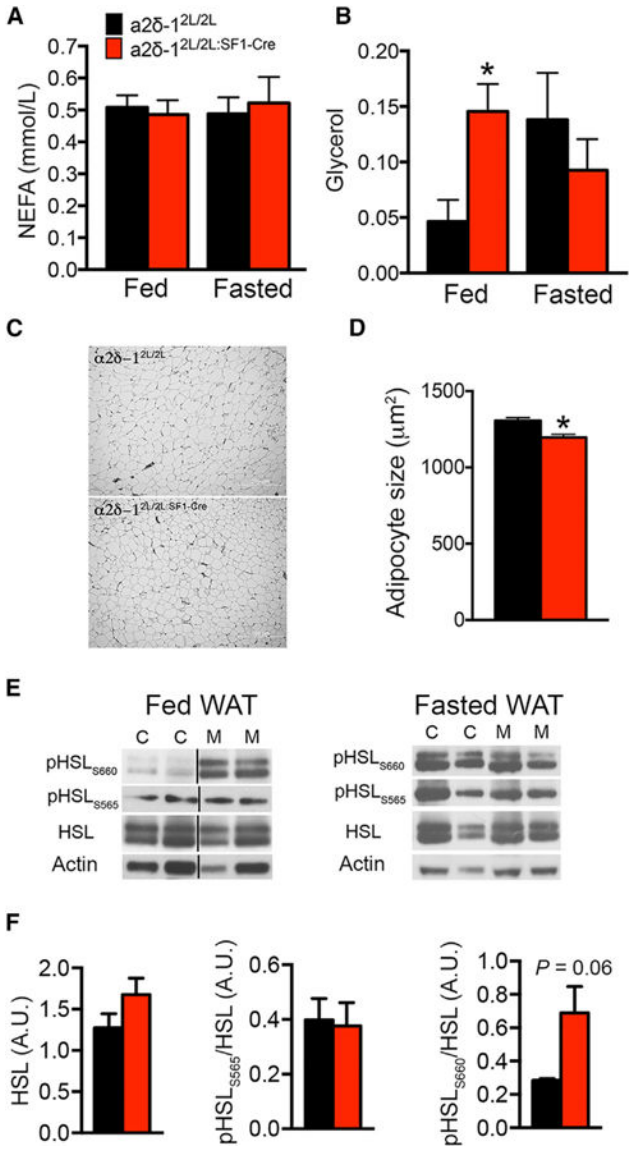

Figure 5. α2δ-1$^{2L/2L:SF1-Cre}$ Mice Exhibit Alterations in Lipolysis

(A) Serum content of NEFA in α2δ-1$^{2L/2L}$ and α2δ-1$^{2L/2L:SF1-Cre}$ mice (fed, n = 7; fasted, n = 5).

(B) Serum levels of glycerol in α2δ-1$^{2L/2L}$ mice (fed, n = 8; fasted, n = 5) and α2δ-1$^{2L/2L:SF1-Cre}$ (fed, n = 9; fasted, n = 4). Two-way ANOVA: feeding status, F(1,22) = 0.43, p = 0.52; genotype, F(1,22) = 0.84, p = 0.37; interaction: F(1,22) = 6.1, p = 0.02. *p = 0.008.

(C) Representative images of white adipose tissue from fed α2δ-1$^{2L/2L:SF1-Cre}$ and α2δ-1$^{2L/2L}$ mice stained with H&E.

(D) Adipocyte size in α2δ-1$^{2L/2L}$ (C) and α2δ-1$^{2L/2L:SF1-Cre}$ (M) mice (n = 3). Two-tailed unpaired t test: *p < 0.0001.

(E) Western blot analysis of pHSL$_{S660}$, pHSL$_{S565}$, HSL, and actin content in WAT of fed and fasted α2δ-1$^{2L/2L}$ and α2δ-1$^{2L/2L:SF1-Cre}$ mice. Black vertical lines indicate splicing of the original blot.

(F) Quantification of western blot analysis in WAT samples obtained from fed $\alpha 2\delta\text{-}1^{2L/2L}$ (n = 3) and $\alpha 2\delta\text{-}1^{2L/2L:SF1\text{-}Cre}$ (n = 5) mice. Two-tailed unpaired t test: #, p = 0.06.
Data are represented as mean ± SEM. See also Figure S6.

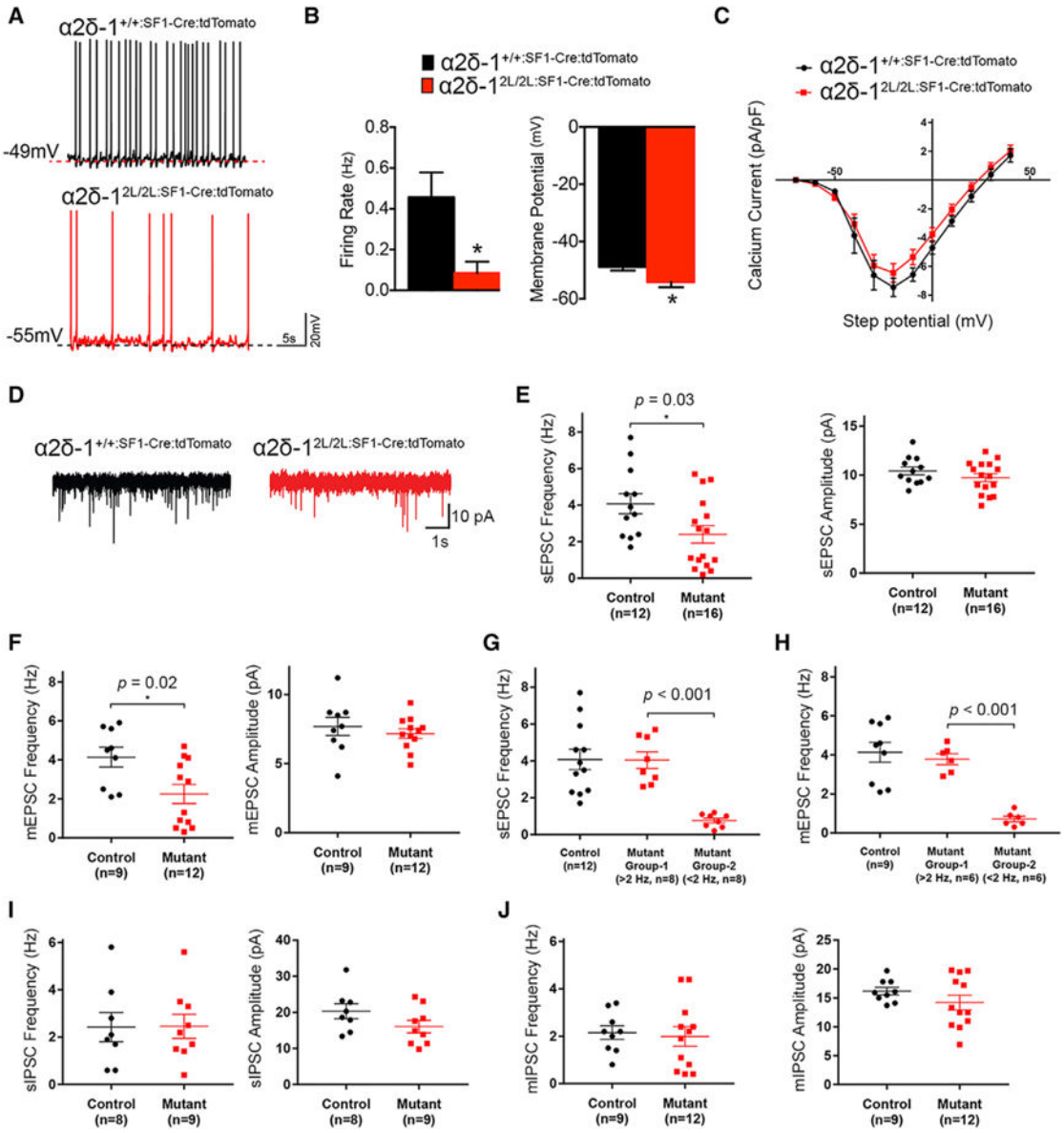

Figure 6. Deletion of α2δ-1 Elicits to Significant Reductions in SF1 Neuronal Activity

(A) Representative traces in current clamp showing SF1 neuronal firing in fed α2δ-1$^{+/+:SF1\text{-}CreTdTomato}$ and α2δ-1$^{2L/2L:SF1\text{-}CreTdTomato}$ mice.

(B) Quantification of spontaneous firing rate (*p = 0.02) and resting membrane potential (*p = 0.04) in SF1 neurons (n = 7–8 cells per group).

(C) Ca^{2+} currents recorded from SF1 cells in α2δ-1$^{+/+:SF1\text{-}CreTdTomato}$ (n = 14 cells) and α2δ-1$^{2L/2L:SF1\text{-}CreTdTomato}$ (n = 10 cells) mice. Current-voltage curve (I-V) relationships resulting from step potentials from −70 mV to −40 mV in 10-mV increments.

(D and E) Representative traces (D) and quantification (E) of sEPSC amplitude and frequency for SF1 neurons in α2δ-1$^{+/+:SF1\text{-}CreTdTomato}$ and α2δ-1$^{2L/2L:SF1\text{-}CreTdTomato}$ mice. *p = 0.03. Two-tailed unpaired t test.

(F) Data of mEPSC amplitude and frequency for SF1 neurons in α2δ-1$^{+/+:SF1\text{-}CreTdTomato}$ and α2δ-1$^{2L/2L:SF1\text{-}CreTdTomato}$ mice. *p = 0.02. Two-tailed unpaired t test.

(G and H) Comparison of sEPSC (G) and mEPSC (H) frequency of putative subpopulations of mutant SF1 neurons.

(I) sIPSC amplitude and frequency for SF1 neurons in $\alpha 2\delta\text{-}1^{+/+:SF1\text{-}CreTdTomato}$ and $\alpha 2\delta\text{-}1^{2L/2L:SF1\text{-}CreTdTomato}$ mice.

(J) mIPSC amplitude and frequency for SF1 neurons in $\alpha 2\delta\text{-}1^{+/+:SF1\text{-}CreTdTomato}$ and $\alpha 2\delta\text{-}1^{2L/2L:SF1\text{-}CreTdTomato}$ mice.

Data are represented as mean ± SEM.

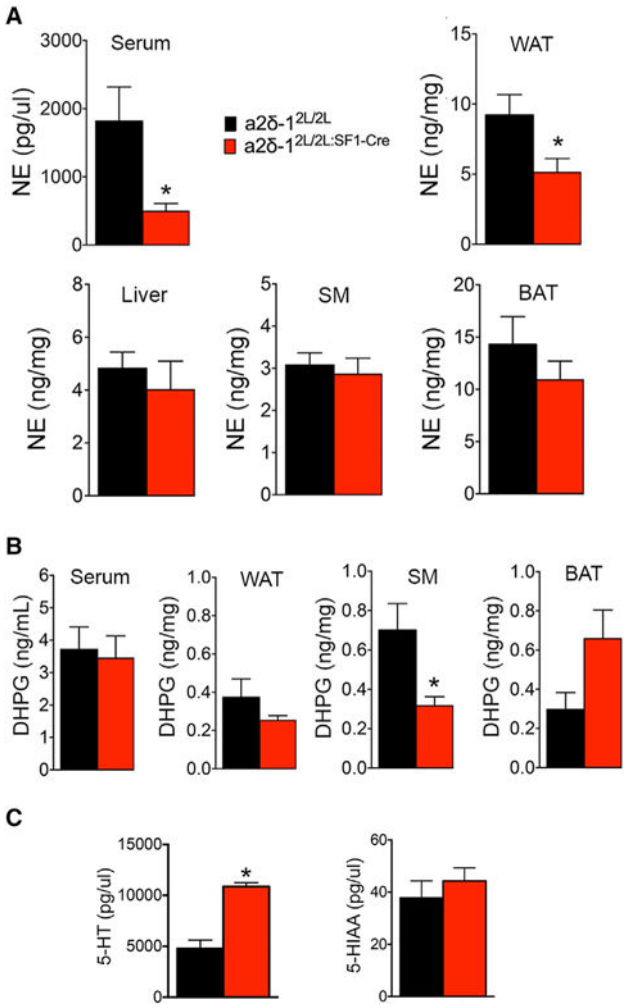

Figure 7. α2δ-1$^{2L/2L:SF1-Cre}$ Mutant Mice Exhibit Reduced Sympathetic Tone and Elevated Levels of Circulating Serotonin

(A) Norepinephrine (NE) content in serum, WAT, liver, skeletal muscle (SM), and brown adipose tissue (BAT) of fed male α2δ-1$^{2L/2L}$ (n = 8) and α2δ-1$^{2L/2L:SF1-Cre}$ (n = 6) mice. Two-tailed unpaired t test, *p = 0.04.

(B) Levels of dihydroxyphenylglycol (DHPG) in serum, WAT, liver, SM, and BAT of fed male α2δ-1$^{2L/2L}$ (n = 7) and α2δ-1$^{2L/2L:SF1-Cre}$ (n = 8) mice. Two-tailed unpaired t test: SM, *p = 0.007.

(C) Serum levels of serotonin (5-HT) and 5-HIAA in fed α2δ-1$^{2L/2L}$ (n = 6) and α2δ-1$^{2L/2L:SF1-Cre}$ (n = 6) mice. Two-tailed unpaired t test: 5-HT, *p < 0.0001.

Data are represented as mean ± SEM.